Photoluminescence of erbium-doped silicon: excitation power dependence

C. A. J. Ammerlaan, D. T. X. Thao, and T. Gregorkiewicz

Van der Waals-Zeeman Institute, University of Amsterdam, Valckenierstraat 65, NL-1018 XE Amsterdam, The Netherlands

N. A. Sobolev

A. F. Ioffe Physicotechnical Institute, Russian Academy of Sciences, 194021 St. Petersburg, Russia
(Submitted January 19, 1999; accepted for publication January 20, 1999)
Fiz. Tekh. Poluprovodn. **33**, 644–648 (June 1999)

The intensity of the photoluminescence of erbium in silicon is analyzed by a model which takes into account the formation of free excitons, the binding of excitons to erbium ions, the excitation of inner-shell $4f$ electrons of erbium ions and their subsequent decay by light emission. Predictions of this model for the dependence of luminescence intensity on laser excitation power are compared with experimental observations. The results for float-zone and Czochralski-grown silicon, in which erbium is introduced by implantation with or without oxygen co-implantation, are remarkably similar. To obtain agreement between model analysis and experimental data it is necessary to include in the model terms describing energy dissipation by an Auger process of both the erbium-bound excitons and the erbium ions in excited state with free electrons in the conduction band. A good quantitative agreement is achieved. © *1999 American Institute of Physics.* [S1063-7826(99)00306-3]

1. INTRODUCTION

The luminescence of rare-earth-doped semiconductors is presently under intense study. In the more fundamentally oriented research, the complex physical processes active in energy transfer from excitation in the entrance channel to light emission in the output channel are investigated. Stimulated by the prospects of practical application of this light source, erbium in silicon, which emits at a wavelength of 1.54 μm, is a prominent system. In a currently accepted model energy fed into the system leads to light emission by erbium ions in a multistep process. Radiation incident on the silicon, with photon energy larger than its bandgap, creates free electrons and holes. Free carriers combine into excitons which can be trapped at the erbium ions. The energy of erbium-bound excitons is transferred to erbium ions and results in excitation of $4f$ core electrons from the $^4I_{15/2}$ ground state into the $^4I_{13/2}$ excited state. The characteristic luminescence is produced upon decay of excited erbium ions. In the present report this chain of processes is analyzed in a mathematical model with the aim of giving a quantitative description.

2. PHOTOLUMINESCENCE MODEL

2a. Energy transfer without Auger processes

The physical model mentioned above, which we examine in this paper, is illustrated in Fig. 1. In a recent paper by Bresler and co-workers the model without the Auger processes has been put on a mathematical basis.[1] A set of rate equations was formulated for free electrons with concentration n, free excitons with concentration n_x, erbium-bound excitons with concentration n_{xb}, and erbium ions in the excited state, with concentration n_{Er}^*. The steady state is described by the balance equations (1)–(4), which we will discuss.

The chain of processes leading to photoluminescence has as the first step the generation of free electrons and holes, to equal concentrations, with rate G by the incident light. Free carriers can combine in a second-order process with rate $\gamma_x n^2$ into free excitons. Trapping of the excitons at erbium sites is proportional to the concentrations of the free excitons and the available free erbium sites. The latter concentration is given as the total concentration of erbium n_{Er} multiplied by the fraction of free sites $[(n_{\mathrm{Er}}-n_{xb})/n_{\mathrm{Er}}]$. The energy is transferred to erbium $4f$ core electrons with a transfer time τ^* but again only to the erbium ions still available in their ground state, i.e., to the fraction $[(n_{\mathrm{Er}}-n_{\mathrm{Er}}^*)/n_{\mathrm{Er}}]$. At high excitation power level these fractions between square brackets tend to zero and lead to saturation of the luminescence output. This manifestation of saturation is related to exhaustion of available erbium centers. Finally, luminescence is produced by the decay with time constant τ_d of erbium ions n_{Er}^* in the excited state. The photon emission rate equal to n_{Er}^*/τ_d is the quantity measured in the experiment.

Reverse processes, as indicated in Fig. 1 by arrows that point to the left, are thermally activated. They include the dissociation of excitons into free electrons and holes fn_x requiring energy gain of E_x, the release of excitons from erbium trapping sites cfn_{xb}, and a back transfer process in which an erbium-bound exciton is recreated from an excited erbium ion. Although these reverse processes hamper the energy transfer toward light emission, they do not remove energy from the chain. The coefficients of forward and reverse processes are related by considerations of detailed balancing.

 © 1999 American Institute of Physics

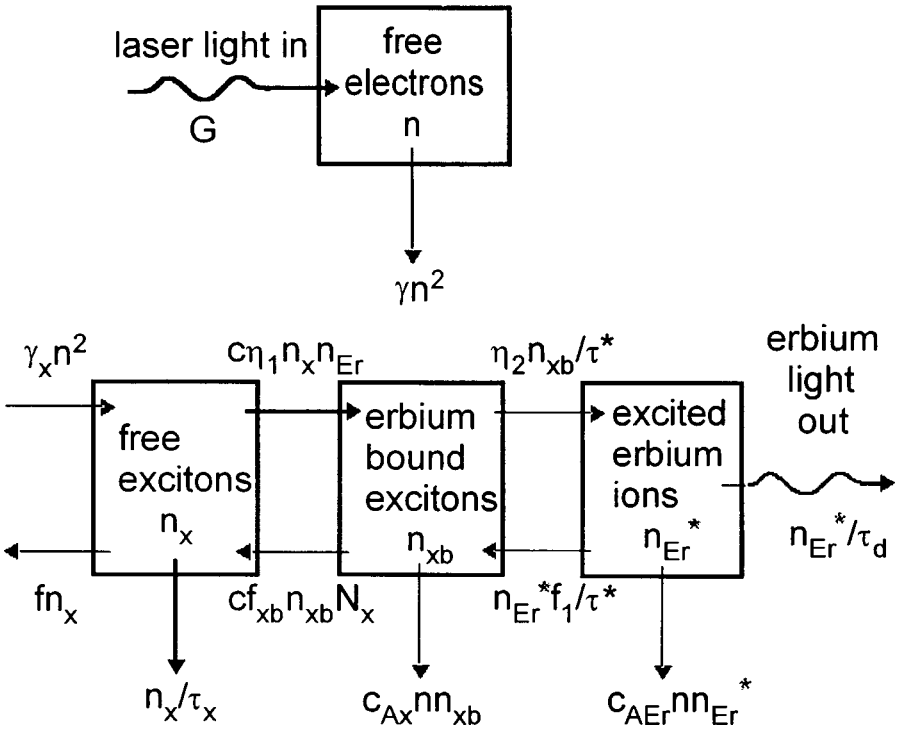

FIG. 1. Two-stream model for the photoexcitation of erbium luminescence showing generation and loss of free electrons n, free excitons n_x, erbium-bound excitons n_{xb}, and erbium ions in the excited state n_{Er}^*. Notation: $\eta_1=(n_{Er}-n_{xb})/n_{Er}$, $\eta_2=(n_{Er}-n_{Er}^*)/n_{Er}$.

Energy is permanently lost by processes which remove energy irreversibly from the chain. Such processes, as indicated in Fig. 1 by vertical arrows downwards, are recombination of electrons and holes via other centers, with the rate γn^2, and recombination of free excitons directly or via alternative centers, n_x/τ_x. The Auger processes represented in Fig. 1 remove energy irreversibly from the luminescence path.

The balance equations based on these processes are

$$G+fn_x=\gamma n^2+\gamma_x n^2, \tag{1}$$

$$\gamma_x n^2+cf_{xb}n_{xb}N_x=cn_x n_{Er}[(n_{Er}-n_{xb})/n_{Er}] + fn_x+n_x/\tau_x, \tag{2}$$

$$cn_x n_{Er}[(n_{Er}-n_{xb})/n_{Er}]+n_{Er}^* f_1/\tau^* =n_{xb}[(n_{Er}-n_{Er}^*)/n_{Er}]/\tau^*+cf_{xb}n_{xb}N_x, \tag{3}$$

and

$$n_{xb}[(n_{Er}-n_{Er}^*)/n_{Er}]/\tau^*=n_{Er}^*/\tau_d+n_{Er}^* f_1/\tau^*. \tag{4}$$

The generation terms are given on the left-hand sides of these equations; loss terms appear in each case on the right-hand side. An exact solution for the equations, in the form of a quadratic equation for n_{Er}^*, is given by Bresler *et al.*[1] The result takes a more simplified form by the restriction to low temperatures, e.g., liquid-helium temperature, when all reverse processes, which require thermal activation, are suppressed. Under these conditions, when $f=f_{xb}=f_1=0$, we obtain

$$a_0(n_{Er}^*/n_{Er})^2-(b_0+b_2G)(n_{Er}^*/n_{Er})+c_2G=0, \tag{5}$$

where

$$a_0=1+cn_{Er}\tau_x[1+(\tau^*/\tau_d)], \tag{5a}$$

$$b_0=1+cn_{Er}\tau_x, \tag{5b}$$

$$b_2=\gamma_x\tau_x c\tau_d[1+(\tau^*/\tau_d)]/\gamma, \tag{5c}$$

and

$$c_2=\gamma_x\tau_x c\tau_d/\gamma. \tag{5d}$$

In general form, the equation predicts saturation of n_{Er}^* at the level $n_{Er}^*/n_{Er}=c_2/b_2$ for high excitation power level G. For low power a linear relationship $n_{Er}^*/n_{Er}=(c_2/b_0)G$ is predicted. In comparing experimental data with these model equations one must be aware that neither generation power nor output luminescence is known very well in absolute numbers. For example, the volume in the sample where excitation takes place is not well defined. For this reason it is useful to eliminate these uncertain factors by resorting to relative units. As regards luminescence intensity, the obvious unit for normalization is the saturation value c_2/b_2. A dimensionless normalized intensity is therefore introduced as $I\equiv(n_{Er}^*/n_{Er})/(c_2/b_2)$. For the excitation power the unit is obtained as the value at which the extrapolated linear increase at low power crosses the saturation level. This occurs at $G_1=b_0/b_2$. The normalized power $P\equiv G/G_1$ is again a dimensionless quantity. In terms of normalized units Eq. (5) is modified to

$$I^2-\alpha(1+P)I+\alpha P=0, \tag{6}$$

where

$$\alpha\equiv b_0b_2/a_0c_2. \tag{6a}$$

It turns out that the dependence of intensity I on generation power P is governed by one parameter α, through which the specific aspects of the luminescence process as a whole are represented. However, from Eq. (6) it is easily concluded

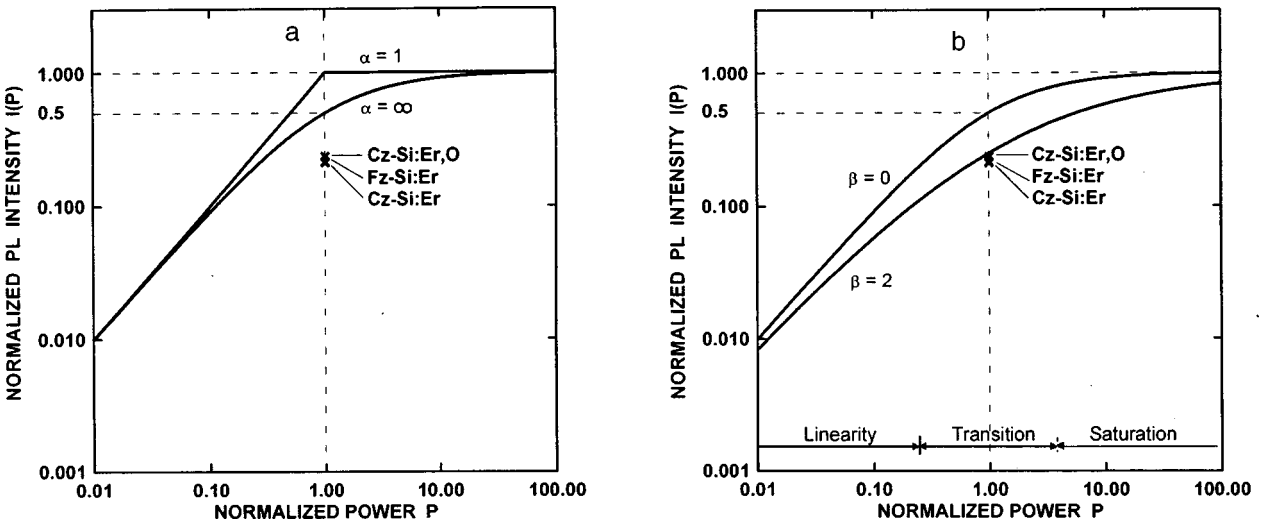

FIG. 2. Normalized luminescence output I plotted as a function of normalized laser power input P; a) for a model without Auger processes, b) for a model including strong Auger decay processes. Experimental data for three samples of type Fz-Si:Er, Cz-Si:Er, and Cz-Si:Er,O are given for unit power $P=1$.

that for low power $I=P$, and for high power $I=1$, irrespective of the value of the parameter α. In normalized form the parameters a_2, b_0, b_2, and c_2 or in basic, more physical form γ, γ_x, c, τ_x, τ^*, and τ_d have no effect on the power dependence in the low and high power regions. Only at intermediate power, i.e., at $P\approx 1$, the results will depend on α. Only in the transition region from linear increase to saturation the observed luminescence provides insight into the luminescence process. The most typical value to study the luminescence mechanism is therefore at power $P=1$. At this level the luminescence intensity is given by

$$I=\alpha-(\alpha^2-\alpha)^{1/2}. \tag{7}$$

From the equality $\alpha=b_0b_2/a_0c_2$ and the parameters as given by Eqs. (5a)–(5d) one concludes that $1\leqslant\alpha\leqslant\infty$. For such values of α solutions from Eq. (7) always exist. For $\alpha=1$ we obtain $I(P=1)=1$ and for $\alpha=\infty$ we have $I(P=1)=0.5$. The range of possible luminescence intensities at unit power $P=1$ is restricted between 0.5 and 1, consistent with Eq. (6). The limiting curves for an extended power range are drawn in Fig. 2a.

Experimental data are also shown in Fig. 2a. They result from measurements at liquid-helium temperature on three samples with different specifications. The sample Fz-Si:Er is float-zoned silicon implanted with erbium. Sample labeled Cz-Si:Er is Czochralski silicon which is similarly implanted. The third sample, labeled Cz-Si:Er,O was codoped with oxygen by implantation. In all cases the luminescence intensity was measured as a function of excitation power. Experimental data are plotted for normalized power $P=1$ at the observed values $I\approx 0.22$. Obviously, this is outside the range of the results as can be described by the model.

2b. Energy transfer with Auger processes

One has to conclude that the presented model cannot give a quantitative description of the luminescence process. In order to improve the model energy losses through Auger processes may be considered, as has been explored before by Palm *et al.*[2] Erbium-bound excitons can dissipate their energy in an Auger process with the involvement of free electrons. Similarly, erbium ions in the excited state can decay in an Auger process also with conduction band electrons. These processes are also shown in Fig. 1. In the balance equations they are implemented by including on the loss side the Auger rates $c_{Ax}nn_{xb}$ and $c_{AEr}nn^*_{Er}$. The extended balance equations for bound excitons and excited erbium ions become

$$cn_xn_{Er}[(n_{Er}-n_{xb})/n_{Er}]+n^*_{Er}f_1/\tau^* = n_{xb}[(n_{Er}-n^*_{Er})/n_{Er}]/\tau^*+cf_{xb}n_{xb}N_x+c_{Ax}nn_{xb}, \tag{8}$$

and

$$n_{xb}[(n_{Er}-n^*_{Er})/n_{Er}]/\tau^*=n^*_{Er}/\tau_d+n^*_{Er}f_1/\tau^*+c_{AEr}nn^*_{Er}. \tag{9}$$

In order to solve the new set of equations (1), (2), (8), and (9) it is helpful to introduce appropriate simplifications. Considering the numerical values, we conclude that the loss of free electrons and holes is dominated by their recombination via traps with the rate γn^2. The loss via exciton formation $\gamma_x n^2$ is comparatively much lower, i.e., $\gamma_x\ll\gamma$. Under such conditions the energy transfer model can be cascaded into two parts. In stream I the balance of electrons is considered separately by Eq. (1). The loss of electrons through exciton formation is ignored in this mainstream. At low temperature this leads to

$$G=\gamma n^2, \tag{10}$$

$$n=(G/\gamma)^{1/2}. \tag{11}$$

The electron concentration obtained from this solution is used to describe the Auger processes. Typical numbers are $G=10^{22}\,\mathrm{cm^{-3}\,s^{-1}}$, $\gamma=10^{-10}\,\mathrm{cm^3\,s^{-1}}$, and $n=10^{16}\,\mathrm{cm^{-3}}$.

In energy stream II the balance of free excitons, bound excitons, and excited erbium ions is considered separately. Solution of the equations leads to a cubic equation in n^*_{Er}/n_{Er}, which, accepting an approximation, can be factorized to yield a quadratic equation

$$(a_0+a_1G^{1/2}+a_2G)(n_{\mathrm{Er}}^*/n_{\mathrm{Er}})^2-(b_0+b_1G^{1/2}+b_2G+b_3G^{3/2})(n_{\mathrm{Er}}^*/n_{\mathrm{Er}})+c_2G=0, \tag{12}$$

where

$$a_0=1+cn_{\mathrm{Er}}\tau_x[1+(\tau^*/\tau_d)], \tag{12a}$$

$$a_1=[(1+cn_{\mathrm{Er}}\tau_x)c_{A\mathrm{Er}}\tau_d+2cn_{\mathrm{Er}}\tau_x\times(\tau^*/\tau_d)c_{A\mathrm{Er}}\tau_d]/\gamma^{1/2}, \tag{12b}$$

$$a_2=cn_{\mathrm{Er}}\tau_x(\tau^*/\tau_d)(c_{A\mathrm{Er}}\tau_d)^2/\gamma, \tag{12c}$$

$$b_0=1+cn_{\mathrm{Er}}\tau_x, \tag{12d}$$

$$b_1=(1+cn_{\mathrm{Er}}\tau_x)(c_{A\mathrm{Er}}\tau_d+c_{Ax}\tau^*)/\gamma^{1/2}, \tag{12e}$$

$$b_2=\{(1+cn_{\mathrm{Er}}\tau_x)c_{A\mathrm{Er}}\tau_d c_{Ax}\tau^*+\gamma_x\tau_x c\tau_d\times[1+(\tau^*/\tau_d)]\}/\gamma, \tag{12f}$$

$$b_3=\gamma_x\tau_x c\tau_d C_{A\mathrm{Er}}\tau_d(\tau^*/\tau_d)/\gamma^{3/2}, \tag{12g}$$

and

$$c_2=\gamma_x\tau_x c\tau_d/\gamma. \tag{12h}$$

At a low power level the model equations reflect the linear increase $n_{\mathrm{Er}}^*/n_{\mathrm{Er}}=(c_2/b_0)G$, just as before. At high power, however, the consistent solution $n_{\mathrm{Er}}^*/n_{\mathrm{Er}}=(c_2/b_3)/G^{1/2}$ predicts decreasing luminescence intensity with increasing excitation source. Such behavior is to be expected since in our case two independent saturation mechanisms are active. The first one drives the concentration of erbium-bound excitons, n_{xb}, toward the concentration of available erbium ions but is limited to stay below or become equal to this concentration. The second saturation mechanism is the combined action of the two Auger processes. At high power, and hence high concentrations of free electrons, the Auger mechanism, which removes excited erbium ions nonradiatively, is very effective. This results in a reduction of n_{Er}^*, which becomes proportional to $1/n$ or $1/G^{1/2}$. Such a decrease has not been observed in our experiments; it has also not been reported in the literature. Inspection of the equations shows that one should expect the decrease to set in at excitation values where $c_{A\mathrm{Er}}\tau_d(\tau^*/\tau_d)(G/\gamma)^{1/2}>1$. Considering the numerical values ($c_{A\mathrm{Er}}\approx 10^{-12}\,\mathrm{cm^3\cdot s^{-1}}$, $\tau^*\approx 10^{-6}\,\mathrm{s}$), this corresponds to high values of G near and above $10^{26}\,\mathrm{cm^{-3}\cdot s^{-1}}$, which are not reached in actual experiments. This can be attributed to the small value of (τ^*/τ_d) since τ^* is in the range of microseconds and τ_d is on the order of several milliseconds. Introducing the approximation $\tau^*/\tau_d\approx 0$, Eqs. (12) reduce in many respects to Eqs. (6). In particular, the term $b_3G^{3/2}$ in Eq. (12) is lost and the equation predicts saturation at c_2/b_2.

For low and for high power levels the solution of Eq. (12) is

$$n_{\mathrm{Er}}^*/n_{\mathrm{Er}}=c_2G/(b_0+b_1G^{1/2}+b_2G). \tag{13}$$

This result is also valid for intermediate power if the Auger processes are strong. Following solution (13), one has saturation at c_2/b_2, linear increase at low power with $(c_2/b_0)G$, and $G_1=b_0/b_2$. Casting Eq. (13) in terms of normalized units, as before, the result will read

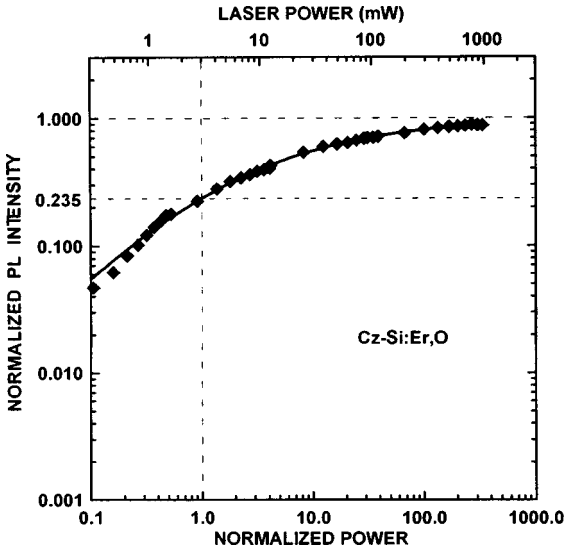

FIG. 3. Photoluminescence intensity, in normalized units I, as a function of applied laser excitation power, both in units G of laser power and in normalized units P for the sample Cz-Si:Er,O. Experimental data points and theoretical curve according to Eq. (14) with the parameter $\beta=2.25$.

$$1=P/(1+\beta P^{1/2}+P), \tag{14}$$

where

$$\beta=b_1/(b_0b_2)^{1/2}, \tag{14a}$$

or

$$\beta=(c_{A\mathrm{Er}}\tau_d+c_{Ax}\tau^*)/\times[c_{A\mathrm{Er}}\tau_d c_{Ax}\tau^*+\gamma_x\tau_x c\tau_d/(1+cn_{\mathrm{Er}}\tau_x)]^{1/2}. \tag{14b}$$

Under the assumed condition of strong Auger effect it reduces to

$$\beta=(c_{A\mathrm{Er}}\tau_d+c_{Ax}\tau^*)/(c_{A\mathrm{Er}}\tau_d C_{Ax}\tau^*)^{1/2}, \tag{14c}$$

or

$$\beta=(c_{A\mathrm{Er}}\tau_d/c_{Ax}\tau^*)^{1/2}+(c_{Ax}\tau^*/c_{A\mathrm{Er}}\tau_d)^{1/2}. \tag{14d}$$

As usual, the power dependence of the luminescence has linear increase at low power with $I=P$ and saturates at high power at $I=1$. Features of the luminescence process are revealed at intermediate power, e.g., at $P=1$, where $I=1/(2+\beta)$. In general, the parameter β will be positive following Eq. (14b); for the case of strong Auger effect $\beta\geqslant 2$, as follows from Eqs. (14c) and (14d). Figure 2b illustrates the curves obtained from Eq. (14) for $\beta=0$ and $\beta=2$. Compared to the previous case, without the Auger effect, the transition region between linear behavior and saturation is broader, because of the appearance of the $P^{1/2}$ term as a result of the Auger effect.

Considering again the experiment, the measured data for the luminescence power dependence for sample Cz-Si:Er,O are plotted in Fig. 3. The solid curve is the best fit using Eq. (14) with the parameter $\beta=2.25$. Similar fits were also made for the samples Fz-Si:Er and Cz-Si:Er; the parameter values are then $\beta=2.63$ and 2.73, respectively.[3] The data points for the three samples for $P=1$ and $I=1/(2+\beta)$ are also plotted in Fig. 2b. The results for the three samples are similar with

$\beta=2.5\pm0.25$. With Eq. (14d) the result is converted to $(c_{A\mathrm{Er}}\tau_d/c_{Ax}\tau^*)^{\pm1}\approx(4\pm1)$. This compares favorably with the data published in the literature, e.g., $c_{A\mathrm{Er}}=10^{-12}\,\mathrm{cm}^3\cdot\mathrm{s}^{-1}$, $\tau_d=10^{-3}\,\mathrm{s}$, $c_{Ax}=10^{-10}\,\mathrm{cm}^3\cdot\mathrm{s}^{-1}$, and $\tau^*=4\times10^{-6}\,\mathrm{s}$ (Ref. 2). From our analysis we conclude that $c_{A\mathrm{Er}}\tau_d/c_{Ax}\tau^*$ is very similar for three kinds of test materials. This can be attributed to an accidental combination of parameters, but one is tempted to believe that all process parameters, i.e., $c_{A\mathrm{Er}}$, τ_d, c_{Ax}, and τ^*, have similar values. In this case the possible difference in structure of the luminescent centers in the three materials has very little influence on the efficiency of the photoluminescence process.

This work was supported in part by the INTAS-RFBR (Grant 95-0531).

[1] M. S. Bresler, O. B. Gusev, B. P. Zakharchenya, and I. N. Yassievich, Phys. Solid State **38**, 813 (1996).
[2] J. Palm, F. Gan, B. Zheng, J. Michel, and L. C. Kimerling, Phys. Rev. B **54**, 17603 (1996).
[3] D. T. X. Thao *et al.* (to be published).

Published in English in the original Russian journal. Reproduced here with stylistic changes by the Translation Editor.